

# The far infrared rotational spectrum of HOBr: line positions and intensities

J. Orphal<sup>a,1,\*</sup>, J.-M. Flaud<sup>a</sup>, Q. Kou<sup>a</sup>, F. Kwabia Tchana<sup>a,b</sup>, O. Pirali<sup>a</sup>

<sup>a</sup>Laboratoire de Photophysique Moléculaire, Centre National de la Recherche Scientifique, UPR 3361, Bât. 350, Centre d'Orsay, 91405 Orsay Cedex, France

<sup>b</sup>Centre de Physique Atomique Moléculaire et Optique Quantique (CEPAMOQ), Université de Douala, B.P. 24157 Douala, Cameroun

Received 2 November 2004; revised 30 November 2004; accepted 4 January 2005

Available online 11 February 2005

This paper is dedicated to Dr. Walter J. Lafferty, for his many contributions to science.

## Abstract

The far infrared absorption spectrum of HOBr has been measured at high resolution between 100 and 400  $\text{cm}^{-1}$  using high-resolution Fourier transform spectroscopy. It was possible to identify not only 1403 pure rotation lines within the vibrational ground state involving levels with rather high  $K_a$  quantum numbers (up to  $K_a=9$ ) but also 457 pure rotation lines within the first excited vibrational state  $3^1$  up to  $K_a=7$ . The ground state lines, combined with 32 microwave transitions available in the literature, were used for a new determination of the rotational constants up to higher orders for both isotopomers  $\text{HO}^{79}\text{Br}$  and  $\text{HO}^{81}\text{Br}$ , by least squares fitting of the observed line positions using a Watson-type Hamiltonian for the calculation of rotational energy levels. In the same way the  $3^1$  rotational lines were fitted together with the few existing microwave transitions and the energy levels derived from the study of the  $\nu_3$  band (J. Orphal, Q. Kou, F. Kwabia Tchana, O. Pirali, and J.-M. Flaud, *J. Mol. Spectrosc.* 221 (2003), 239–243) leading to an improved set of Hamiltonian constants. Finally relative line intensities were measured and used for the determination of rotational corrections to the  $b$ -component of the permanent dipole moment. © 2005 Elsevier B.V. All rights reserved.

**Keywords:** HOBr; Hypobromous acid; Infrared; High resolution; Line positions; Line intensities

## 1. Introduction

HOBr plays an important role in atmospheric chemistry [1–6]. It is formed in the stratosphere by the gas-phase reaction between the BrO and  $\text{HO}_2$  radicals and by heterogeneous reactions of  $\text{BrONO}_2$  with  $\text{H}_2\text{O}$  on Polar Stratospheric Cloud particles. In the stratosphere, HOBr is rapidly photolyzed by sunlight [7–9] releasing OH and Br radicals that destroy ozone in catalytic cycles [10]. In the troposphere, HOBr is formed by reactions including heterogeneous chemistry on sea salt aerosols, and—in addition to photolysis and gas-phase reactions—can be removed from the gaseous phase by dissolution in aqueous aerosol particles [11–15]. In the chemical cycles of

tropospheric bromine, HOBr is one of the most important intermediates [4,5,16].

However, atmospheric detection of HOBr is still difficult because of its rather low concentrations. Its sharp rotational  $Q$ -branches in the far-infrared region have been used to estimate an upper limit of 2.8 ppt for the HOBr mixing ratio in the stratosphere, using balloon-borne limb-sounding of atmospheric emission [17]. HOBr is also one of the target species of the SAFIRE-A remote-sensing experiment on the Geophysika M-55 high-altitude aircraft [18], and it is part of the potential scientific data products of future space-borne microwave limb-sounders [19]. With the increasing sensitivity of far-infrared instruments, the observation of atmospheric HOBr might become feasible in the future.

From the spectroscopic point of view, the electronic ground and excited states of HOBr have been characterized by several high-level ab-initio calculations [20–26], and the ground electronic state has been studied (together with DOBr) in the microwave region [27] as well as by high-resolution Fourier-transform infrared spectroscopy

\* Corresponding author. Tel.: +33 1 6915 7528; fax: +33 1 6915 7530.

E-mail address: [orphal@lisa.univ-paris12.fr](mailto:orphal@lisa.univ-paris12.fr) (J. Orphal).

<sup>1</sup> New address: Laboratoire Interuniversitaire de Systèmes Atmosphériques (LISA), CNRS URM 7583, Faculté des Sciences et Technologie, 61 avenue du Général de Gaulle, 94010 Créteil Cedex, France.

and rotational analysis of the fundamental bands  $\nu_1$ ,  $\nu_2$  and  $\nu_3$  around 3615, 1163 and 620  $\text{cm}^{-1}$ , respectively [28–30].

In this paper, we present the first high-resolution absorption measurements of the pure rotational spectrum of HOBr in the far infrared region between 100 and 400  $\text{cm}^{-1}$ . A total of 1403 pure rotation lines within the ground state involving levels with rather high  $K_a$  quantum numbers (up to  $K_a=9$ ) were observed and assigned. From these lines, together with 32 microwave transitions available in the literature [28], a set of new rotational and centrifugal distortion constants of the ground states was determined for both the HO<sup>79</sup>Br and HO<sup>81</sup>Br isotopomers. Also a total of 457 rotation lines within the first excited vibrational 3<sup>1</sup> state were measured up to  $K_a=7$ . They were fitted together with the few existing microwave lines and the energy levels derived from the analysis of the  $\nu_3$  band [30] leading to an improved set of Hamiltonian constants. Finally measurements of individual line intensities for 585 lines were used to determine the rotational corrections to the  $b$ -component of the permanent transition moment.

## 2. Experimental

The experimental procedure has already been described in a previous paper [30]. To give only the most important facts: the far-infrared spectrum of HOBr was measured using a commercial Bruker IFS-120 HR Fourier-transform spectrometer, together with a White-type multi-pass absorption cell made of Pyrex glass, with gold-coated mirrors and equipped with polyethylene windows. The optical path length in the cell was adjusted to 400 cm (4 passes). The beamsplitter used was a 6  $\mu\text{m}$  mylar foil, the broadband light source was a glowbar inside of the Bruker IFS-120 HR source chamber, and the detector was a He-cooled bolometer. The spectral resolution was 0.0032  $\text{cm}^{-1}$

(Full-Width at Half-Maximum FWHM), and the free spectral range was limited to 0–1128  $\text{cm}^{-1}$ . The observed linewidth for unblended lines was about 0.005  $\text{cm}^{-1}$  (FWHM).

HOBr was synthesized by flowing slowly gaseous bromine over dry yellow HgO powder, yielding gaseous Br<sub>2</sub>O and significant amounts of HOBr by heterogeneous reactions with residual H<sub>2</sub>O adsorbed on the cell's surfaces. The total pressure in the absorption cell was adjusted to 7 mbar, including Br<sub>2</sub>O, HOBr, and residual Br<sub>2</sub>. Spectra were recorded in blocks of 10 scans, each taking approximately 2 h. It was observed that the HOBr sample slowly decomposed inside the cell, reaching nearly zero absorption after 12 h. In order to minimize the effects of sample decomposition on the determination of relative line intensities, only the first block of data was used for the analysis described below.

Fig. 1 shows an overview of the recorded spectrum at high resolution. Note that, besides HOBr, there is absorption by residual H<sub>2</sub>O inside the cell and the interferometer. In addition, weak absorptions due to the rotational spectrum of HOCl [31], probably resulting from an impurity in the chemical synthesis, were observed. Figs. 2, 3 and 4 show more details of the spectra. The signal/noise ratio is about 100 (root mean square, RMS), but significantly decreasing towards lower wavenumbers. Note that for the line intensity determinations, the spectrum was slightly apodized using the Norton-Beer 'medium' apodization function, to minimize the effects of the instrumental line shape (see Fig. 5). All line positions were determined using the Bruker OPUS software peakfinder routine, and were calibrated to absolute vacuum wavenumbers using the residual H<sub>2</sub>O lines and the line positions of Ref. [32] recommended by the IUPAC [33]. The experimental uncertainty of the calibrated line positions is 0.00026  $\text{cm}^{-1}$  (RMS deviation of 66 rotational lines of H<sub>2</sub>O between 100–400  $\text{cm}^{-1}$ ).

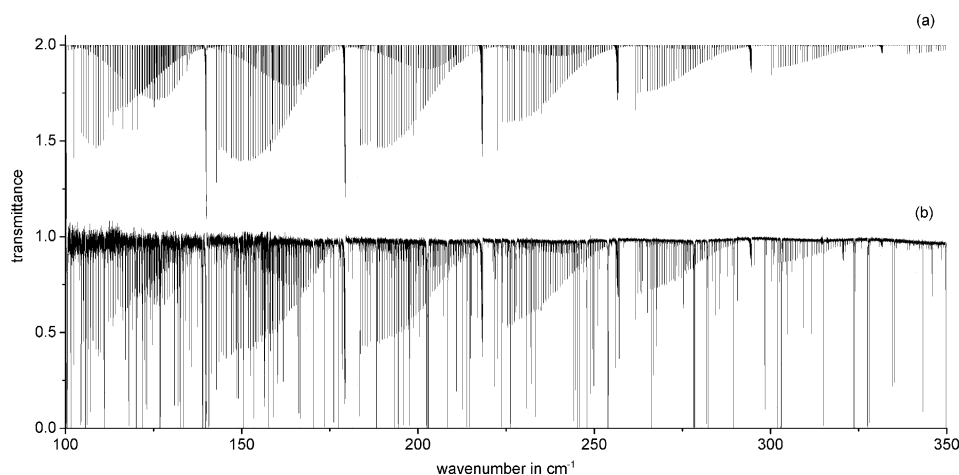


Fig. 1. Overview of the measured absorption spectrum of HOBr. The spectral resolution is 0.0032  $\text{cm}^{-1}$ , the absorption path is 800 cm. One can see the distinct R-branches for different  $K_a$  values.

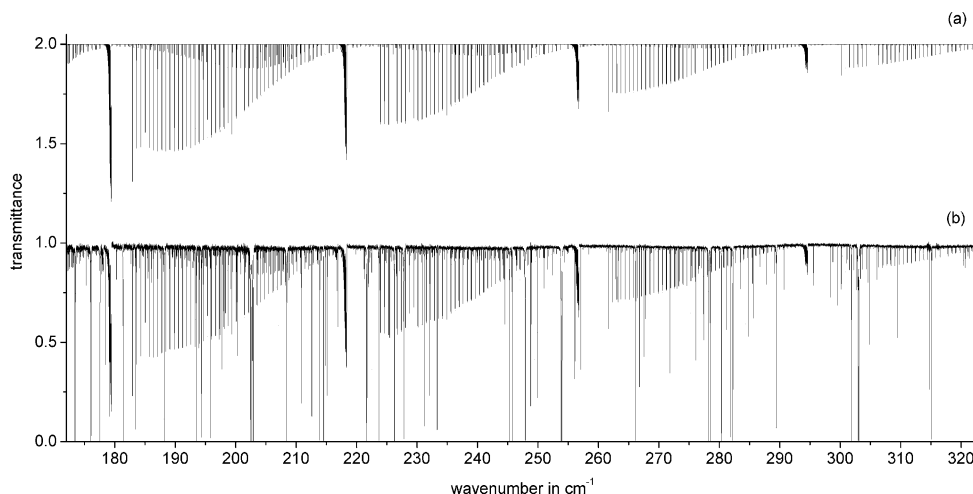


Fig. 2. A portion of the observed spectrum between in the 165–325  $\text{cm}^{-1}$  range. The sharp  $Q$ -branches and strong  $R$ -branches are clearly visible, while the  $P$ -branches are much weaker. The upper trace (a) shows the modelled spectrum and the lower trace (b) shows the observed spectrum. Strong lines that are not reproduced in the modelled spectrum are due to residual water vapour within the cell and in the interferometer.

### 3. Analysis

#### 3.1. Line positions and energy levels

The assignment process of the pure rotation spectra of both isotopic species was straightforward. Starting from the molecular constants of Ref. [29], lines up to  $J$  and  $K_a$  values of about 40 and 6 were easily assigned for the ground state. The constants were then refined by a non-linear least-squares fit using a Watson-type  $A$ -reduced Hamiltonian in the  $F'$  representation [34], and the refined constants were used to predict new line positions which allowed further assignments. New line assignments were performed by comparing the observed spectrum with synthetic spectra based on the preliminary rotational constants obtained from the refinements. The process was repeated liberating successively higher-order constants (in particular required

for transitions with higher  $K_a$ ) until no new assignments were possible. As a result, the far-infrared lines observed in the present work between 100 and 360  $\text{cm}^{-1}$  have a better coverage of high  $K_a$  values (up to 9, see Table 1) than what was achieved in a previous study [29] using only microwave transitions and ground-state combination differences from the mid-infrared bands  $\nu_1$  and  $\nu_2$ . In the final calculations, the observed lines from this work were combined with the microwave data from Ref. [27] and fitted using a Watson-type  $A$ -reduced Hamiltonian in the  $F'$  representation [34]. In order to include the microwave data, we have recalculated the individual line centers without quadrupole splitting using the rotational and higher-order constants of Ref. [27], and for correctly weighting the microwave and new infrared transitions in a simultaneous fit, the inverse of the squared uncertainties was used (50 KHz and 9 MHz, respectively). It is interesting to note that, because high  $K_a$  levels were

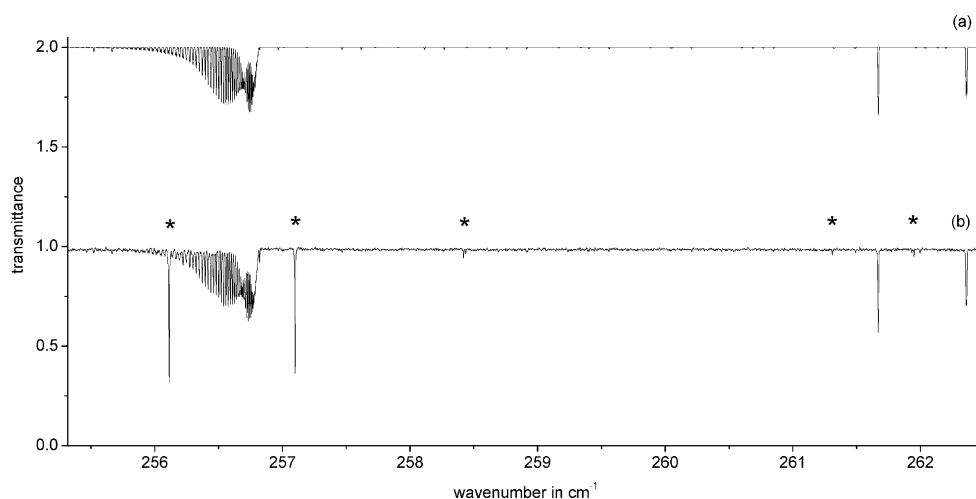


Fig. 3. A portion of the observed spectrum between in the 255–263  $\text{cm}^{-1}$  range (transitions with  $K_a=7-6$ ). The upper trace (a) shows the modelled spectrum and the lower trace (b) shows the observed spectrum. Note that the  $Q$ -branches of  $\text{HO}^{79}\text{Br}$  and  $\text{HO}^{81}\text{Br}$  overlap strongly around 256.6  $\text{cm}^{-1}$ . Lines marked with an asterisk are due to residual  $\text{H}_2\text{O}$ .

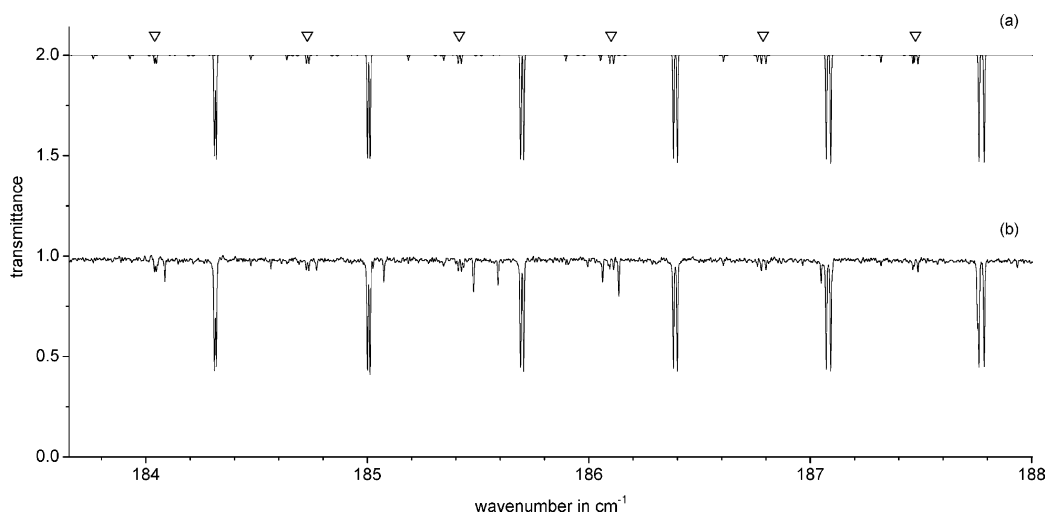


Fig. 4. A portion of the observed spectrum between in the 184–188  $\text{cm}^{-1}$  range ( $R$ -branch transitions with  $K_a=4$ –5). The upper trace (a) shows the modelled spectrum and the lower trace (b) shows the observed spectrum. Note that the rotational transitions of the  $\text{HO}^{79}\text{Br}$  and  $\text{HO}^{81}\text{Br}$  species with the same quantum numbers are always very close due to the similarity of the rotational constants (see also Table 2). Lines marked with a triangle are due rotational transitions within the  $3^1$  state of HOBr. Lines that are not reproduced in the modelled spectrum are due to residual  $\text{H}_2\text{O}$ .

observed, it has been possible for the first time to determine all diagonal sextic centrifugal distortion constants, two off-diagonal sextic constants, and even the octic constant  $P_K$ , see Table 2.

Also the assignment process of the rotation spectrum within the  $3^1$  vibrational states of both isotopic species (see the lines indicated by triangles in Fig. 4) proved to be rather easy starting from the rotational constants derived from the analysis of the  $\nu_3$  band [30]. However we had to refine the constants in order to assign lines with rather high  $K_a$  (up to 7) quantum numbers since in the previous study only lines with  $K_a \leq 4$  were observed. It is worth stressing that this new study has led to a much better determination of

the  $X_K$  constants and in particular of the sextic constant  $H_K$  (See Table 2).

### 3.2. Line intensities

To determine the relative line intensities of the rotational transitions of HOBr in the far-infrared region, a non-linear least-squares fitting routine was used that minimises the differences between the observed and modelled spectra by adjusting the line positions and intensities together with two parameters for the baseline (offset and tilt). An example for the quality of the fitting procedure is given in Fig. 5 for the  $20_{5,16}$ – $19_{4,15}$ / $20_{5,15}$ – $19_{4,16}$  transitions of  $\text{HO}^{79}\text{Br}$  and  $\text{HO}^{81}\text{Br}$ . Note that the line widths were determined only once from fitting of a few selected transitions with high signal/noise ratio and then kept fixed during the entire analysis, to minimize the influence of systematic errors, in particular for the many overlapping lines in the low wavenumber region. All fits were inspected visually for quality and fits with bad residuals or high correlations between line parameters (in particular for overlapping lines) were rejected from the further analysis procedure. Finally, a

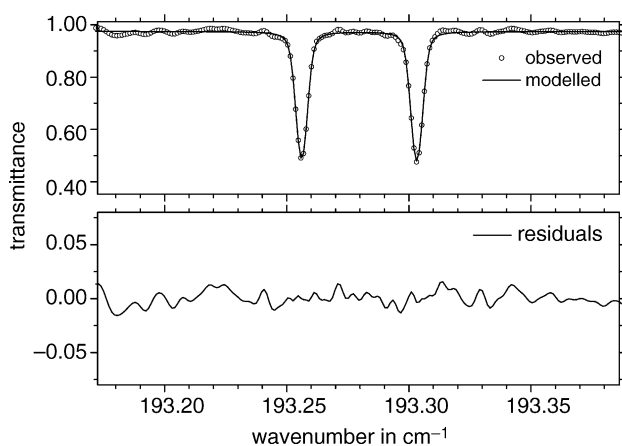


Fig. 5. The  $20_{5,16}$ – $19_{4,15}$ / $20_{5,15}$ – $19_{4,16}$  transitions of  $\text{HO}^{79}\text{Br}$  and  $\text{HO}^{81}\text{Br}$ . The line at the left is due to  $\text{HO}^{81}\text{Br}$ , the line at the right is due to  $\text{HO}^{79}\text{Br}$ . The asymmetry splittings between the  $20_{5,16}$ – $19_{4,15}$  and  $20_{5,15}$ – $19_{4,16}$  transitions (predicted from the energy calculations) are less than  $10^{-5} \text{ cm}^{-1}$ . The open circles are the observed spectrum, the straight line in the upper plot is the modelled spectrum from the non-linear least-squares fit to determine the individual line intensities, and the straight line in the lower plot is the difference between the observed and modelled data.

Table 1  
Range of observed ground state energy levels

$K_a$	$\text{HO}^{81}\text{Br}$		$\text{HO}^{79}\text{Br}$	
	$J_{\min}$	$J_{\max}$	$J_{\min}$	$J_{\max}$
2	7	49	16	49
3	4	50	3	50
4	4	55	4	55
5	6	56	5	56
6	7	51	6	51
7	8	47	8	47
8	9	27	9	27
9	11	21	10	21

Table 2  
Rotational constants of the ground and  $v_3=1$  states of HOBr (A-reduction, I<sup>a</sup>)

Constant	HO <sup>81</sup> Br		HO <sup>79</sup> Br	
	Ground State	$v_3=1$	Ground state	$v_3=1$
$E$	0.0	618.90605 (55)	0.0	620.22850 (57)
$A$	20.4700384 (760)	20.4407086 (250)	20.4701657 (770)	20.4408104 (200)
$B$	0.35127762 (580)	0.34840754 (170)	0.35281792 (350)	0.34992867 (140)
$C$	0.34483688 (580)	0.34200048 (210)	0.34632149 (450)	0.34346658 (190)
$\Delta_K \times 10^2$	0.4606577 (2600)	0.4585781 (1200)	0.460741 (1400)	0.45866671 (9700)
$\Delta_{JK} \times 10^4$	0.2488014 (3800)	0.2455408 (5300)	0.250389 (3100)	0.2471408 (4800)
$\Delta_J \times 10^6$	0.4265380 (7200)	0.432802 (2000)	0.429834 (4700)	0.434306 (1200)
$\delta_K \times 10^4$	0.10110 (2900)	0.10110 <sup>a</sup>	0.10110 <sup>b</sup>	0.10110 <sup>a</sup>
$\delta_J \times 10^8$	0.639190 (6400)	0.639190 <sup>a</sup>	0.70493 (500)	0.70493 <sup>a</sup>
$H_K \times 10^5$	0.52381 (1200)	0.524395 (1500)	0.52716 (3500)	0.527384 (1300)
$H_{KJ} \times 10^7$	0.186045 (1400)	0.18988 (1000)	0.1780 (1300)	0.17972 (1000)
$H_{JK} \times 10^{10}$	0.3896 (1500)	0.3896 <sup>a</sup>	0.3896 <sup>b</sup>	0.3896 <sup>a</sup>
$H_J \times 10^{12}$	−0.3003 (2000)	−0.3003 <sup>a</sup>	−0.3003 <sup>b</sup>	−0.3003 <sup>a</sup>
$L_K \times 10^7$	−0.11328 (2000)	−0.11328 <sup>a</sup>	−0.11580 (2400)	−0.11580 <sup>a</sup>
$L_{KKJ} \times 10^{10}$	−0.5348 (1700)	−0.5348 <sup>a</sup>	−0.4057 (2000)	−0.4057 <sup>a</sup>
$P_K \times 10^{10}$	0.2002 (1100)	0.2002 <sup>a</sup>	0.2002 <sup>b</sup>	0.2002 <sup>a</sup>
$J$ range	4–56	1–41	4–56	2–39
$K_a$ range	0–9	0–7	0–9	0–7
No. of lines	746 FIR + 16 MW	225 FIR + 370 IR + 3 MW	657 FIR + 16 MW	232 FIR + 452 IR + 4 MW
RMS IR	0.0006 cm <sup>−1</sup>	0.0008 cm <sup>−1</sup>	0.0004 cm <sup>−1</sup>	0.0008 cm <sup>−1</sup>
RMS MW	33 kHz	11 kHz	43 kHz	8 kHz

Note: All values, except  $J$  and  $K_a$  range, ‘No. of lines’ and ‘RMS MW’ are given in cm<sup>−1</sup>.

<sup>a</sup> Constant fixed to the ground-state value.

<sup>b</sup> fixed to the same value for both isotopomers.

total of 585 individual line intensities were obtained in this way (260 for HO<sup>79</sup>Br and 325 for HO<sup>81</sup>Br).

For the theoretical analysis, it has to be remembered that the intensity of a line (in cm<sup>−1</sup>/ (molecule cm<sup>−2</sup>)) is given by the expression [35]

$$k_\nu^N = \frac{8\pi\nu}{4\pi\epsilon_0 3hcZ(T)} \left( 1 - \exp\left(-\frac{hc\nu}{kT}\right) \right) \exp\left(-\frac{hcE_A}{kT}\right) R_A^B,$$

where  $\nu$  is the wavenumber of the transition,  $E_A$  is the energy of the lower state  $A$ ,  $Z(T)$  is the partition function, and  $R_A^B$  is the matrix element of the transition moment operator. This transition moment operator can be expanded [35] with respect to the direction cosines and the components  $J_a$  of the total angular momentum  $J$ . Its matrix elements were calculated between the eigenfunctions derived from the diagonalization of the Hamiltonian matrices. The fittings of the experimental line intensities of HO<sup>79</sup>Br and HO<sup>81</sup>Br were first performed separately for each species but, since they led to transition moment parameters consistent to within their estimated accuracies, it was decided to fit the lines of the two isotopologues with the same transition moment expansion. It is worth noting that, since the amount of HOBr in the cell was not known, only relative line intensities were measured, and consequently only the rotational corrections to the permanent dipole moment were determined.

Consequently all the transition moment parameters were scaled to the permanent dipole moment measured by Stark effect [27] and the corresponding rotational corrections to the permanent transition moment are given in Table 3. This

also leads to a determination of the HOBr concentration in the absorption cell,  $7.0 \times 10^{14}$  molecules/cm<sup>3</sup>, which is close to the value obtained by *Deters et al.* [7] ( $3.9 \times 10^{14}$  molecules/cm<sup>3</sup>) who investigated the ultraviolet-visible spectrum of HOBr using the same chemical synthesis. This allows furthermore to determine the integrated band strength of the  $v_3$  bands around 620 cm<sup>−1</sup> at 296 K [30],  $4.17 \times 10^{-19}$  cm<sup>−1</sup>/ (molecule cm<sup>−2</sup>) equivalent to 10.2 cm<sup>−2</sup>/atm or 2.51 km/mole [36] for each HOBr isotopologue (in good agreement with the ab-initio value of 2.26 km/mole [25]), with an accuracy of about 20%, the main contribution to the overall uncertainty being the relatively low signal/noise ratio around 620 cm<sup>−1</sup>. Finally when looking at Table 3 it is clear that the rotational lines intensities are subject to strong rotational corrections; such an effect being also obvious in Fig. 6. Note that a strong Herman-Wallis effect was also observed for the  $b$ -type transitions in the  $\nu_1$  band of HOBr [29].

No correction for the effects of thermal sample and window radiation has been made for the intensity

Table 3  
Transition moment constants for the pure rotational spectrum of HOBr

Operator	HO <sup>79</sup> Br/HO <sup>81</sup> Br	
	C-m	Debye
$\phi_x$	$-4.617 \times 10^{-30}$	$-1.384 \times 10^{-00}$
$\{i\phi_y, J_z\}$	$1.91 (33) \times 10^{-31}$	$5.73 (100) \times 10^{-02}$
$\{\phi_z, iJ_y\}$	$-3.582 (333) \times 10^{-33}$	$-1.074 (100) \times 10^{-03}$
$\{\phi_x, J_z^2\}$	$-2.351 (287) \times 10^{-32}$	$-7.049 (860) \times 10^{-03}$
$\{\phi_x, J^2\}$	$-1.983 (120) \times 10^{-34}$	$-5.946 (360) \times 10^{-05}$

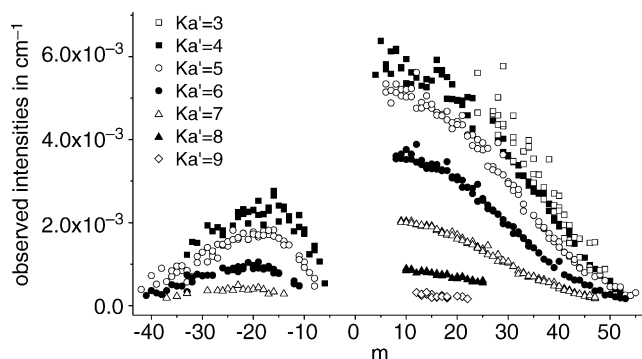


Fig. 6. Observed relative line intensities in the far-infrared rotational spectrum of HOBr determined from non-linear least squares fits of 585 individual lines. All transitions of HO<sup>79</sup>Br and HO<sup>81</sup>Br are presented together. Note that for the low- $K_a$  transitions the noise is larger than at higher  $K_a$  values, which is due to the reduced signal/noise ratio around 100 cm<sup>-1</sup> (see also Fig. 1).

determination, which leads to a possible systematic increase of the relative linestrength of weak lines of up to 3% (see also Ref. [31]). In order to validate the observed line-strengths of HOBr we have compared the observed lines of water vapour within the cell with the intensities of the HITRAN database [37], covering the same range of observed intensities as for HOBr, yielding a straight line with an RMS of 8% (see Fig. 7). The effects of sample emission are therefore validated to be smaller than 8%, but are probably even less than 3% (see Ref. [31]).

Using the rotational constants gathered in Table 2 and the dipole moment expansion of Table 3 a linelist of the far-infrared spectrum of HOBr has been generated. It includes not only the pure rotational transitions within the ground vibrational state but also the rotational transitions within the first excited vibrational state 3<sup>1</sup>, and reproduces very well the observed spectrum (see Figs. 2, 3 and 4). Note that for the 3<sup>1</sup> state it was assumed that the transition moment was

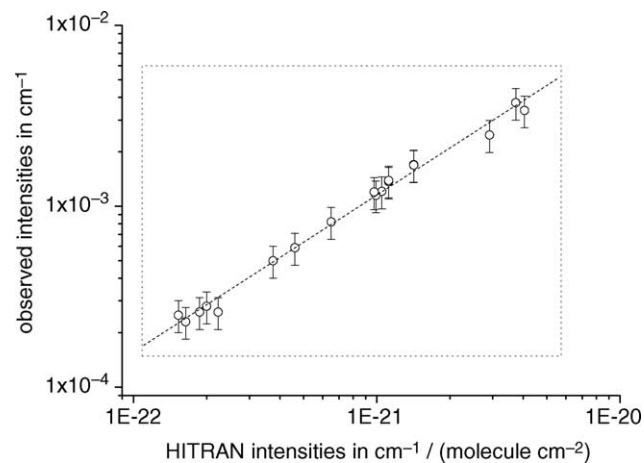


Fig. 7. Observed relative H<sub>2</sub>O line intensities in the far-infrared compared to the line intensities in the HITRAN database [36]. The good agreement indicates negligible contributions due to sample emission, within the range of observed HOBr relative intensities. The straight line is a fit yielding a correlation coefficient of 98% and an RMS deviation of 8%.

the same as for the ground vibrational state, although the observed rotational transitions within the 3<sup>1</sup> state are slightly stronger than the modelled ones. However due to its weakness the latter effect is of negligible influence to the pure rotational spectrum in this spectral region (see Fig. 4).

#### 4. Conclusion

The far-infrared rotational spectrum of hypobromous acid HOBr was measured by high-resolution Fourier-transform absorption spectroscopy. From the analysis of over 1900 lines involving higher  $K_a$  and  $J$  values than observed previously, accurate rotational and centrifugal distortion constants have been derived for the ground and 3<sup>1</sup> vibrational states of HO<sup>79</sup>Br and HO<sup>81</sup>Br. Also individual line intensities have been measured and were used to determine the rotational corrections to the permanent dipole moment of HOBr. The new Hamiltonian and dipole moment constants were used to calculate a synthetic linelist suitable for atmospheric remote-sensing using high-resolution spectroscopy in the far infrared.

#### Acknowledgements

The authors wish to thank Dr. K. V. Chance (Harvard-Smithsonian Astrophysical Observatory, USA) for use of his line fitting programme SPECFIT, and Dr. H. S. P. Müller (University of Köln, Germany) for helpful discussions. Financial support by the 'Programme National de Chimie Atmosphérique' (PNCA, France) is gratefully acknowledged.

#### References

- [1] B.J. Finlayson-Pitts, F.E. Livingston, H.N. Berko, *Nature* 343 (1990) 622–625.
- [2] R. Vogt, P.J. Crutzen, R. Sander, *Nature* 383 (1996) 327–330.
- [3] W.J. Bloss, D.M. Rowley, R.A. Cox, R.L. Jones, *Phys. Chem. Chem. Phys.* 4 (2002) 3639–3647.
- [4] R. Glasow, R. Kuhlmann, M. Lawrence, U. Platt, P. Crutzen, *Atm. Chem. Phys. Discuss.* 4 (2004) 4877–4913.
- [5] R. Sander, W. Keene, A. Pszenny, R. Arimoto, G. Ayers, E. Baboukas, J. Cainey, P. Crutzen, R. Duce, G. Hönninger, B. Huebert, W. Maenhaut, N. Mihalopoulos, V. Turekian, R. Van Dingenen, *Atm. Chem. Phys.* 3 (2003) 1301–1336.
- [6] J.P.D. Abbatt, G.C.G. Waschewsky, *J. Phys. Chem. A* 102 (1998) 3719–3725.
- [7] B. Deters, S. Himmelmann, C. Blindauer, P. Burrows, *Ann. Geophys.* 14 (1996) 468–475.
- [8] O.V. Rattigan, D.J. Lary, R.L. Jones, R.A. Cox, *J. Geophys. Res.*, D 101 (1996) 23021–23025.
- [9] T. Ingham, D. Bauer, J. Landgraf, J.N. Crowley, *J. Phys. Chem. A* 102 (1998) 3293–3301.
- [10] The World Meteorological Organization, *Global Ozone Research and Monitoring Project, Report No. 44, Scientific Assessment of Ozone*

- Depletion*: 1998, edited by NOAA, NASA, UNEP, WMO, and CEC, 1999.
- [11] A. Allan, R. Oppliger, M.J. Rossi, *J. Geophys. Res.*, D 102 (1997) 23529–23541.
- [12] U. Kirchner, T. Benter, R.N. Schindler, J. Hirokawa, K. Onaka, Y. Kajii, H. Akimoto, *Ber. Bunsenges. Phys. Chem.* 101 (1997) 975–977.
- [13] S. Fickert, J.W. Adams, N. Crowley, *J. Geophys. Res.*, D 104 (1999) 23719–23727.
- [14] N. Lahoutifard, P. Lagrange, J. Langrange, S.L. Scott, *J. Phys. Chem. A* (2002) 11891–11896.
- [15] M. Wachsmuth, H.W. Gaggeler, R. von Glasow, M. Ammann, *Atmos. Chem. Phys. Discuss.* 2 (2002) 1–28.
- [16] R. von Glasow, R. Sander, A. Bott, P.J. Crutzen, *J. Geophys. Res.*, D 107 (2002) 4341–4357.
- [17] D.G. Johnson, W.A. Traub, K.V. Chance, K.W. Jucks, *Geophys. Res. Lett.* 22 (1995) 1373–1376.
- [18] B. Carli, P.A.R. Ade, U. Cortesi, P. Dickinson, M. Epifani, F.C. Gannaway, A. Gignoli, C. Keim, C. Lee, J. Leotin, F. Mencaraglia, A.G. Murray, I.G. Nolt, M. Ridolfi, *J. Atm. Ocean. Technol.* 16 (1999) 1313–1328.
- [19] J. Urban, Sub-mm Limb-sounding of Earth's Atmosphere: Optimal Spectral Band Selection for Measuring Species with Weak Spectral Signatures, EGS XXV General Assembly, Nice, France, 2000.
- [20] T.J. Lee, S. Parthiban, M. Head-Gordon, *J. Phys. Chem.* 99 (1995) 15074.
- [21] P. Palmieri, C. Puzzarini, R. Tarroni, *Chem. Phys. Lett.* 256 (1996) 409.
- [22] J.S. Francisco, M.R. Hand, I.H. Williams, *J. Phys. Chem.* 100 (1996) 9250.
- [23] K.A. Peterson, *Spectrochim. Acta A* 53 (1997) 1051.
- [24] T.J. Lee, S. Parthiban, M. Head-Gordon, *Spectrochim. Acta A* 55 (1999) 561.
- [25] K.A. Peterson, *J. Chem. Phys.* 113 (2000) 4598–4612.
- [26] C.M.P. Santos, R.B. Faria, J.O. Machuca-Herrera, S. de P. Machado, *Can. J. Chem.* 79 (2001) 1135–1144.
- [27] Y. Koga, H. Takeo, S. Kondo, M. Sugie, C. Matsumura, G.A. McRae, E.A. Cohen, *J. Mol. Spectrosc.* 138 (1989) 467–481.
- [28] G.A. McRae, E.A. Cohen, *J. Mol. Spectrosc.* 139 (1990) 369–376.
- [29] E.A. Cohen, G.A. McRae, T.L. Tan, R.R. Friedl, J.W.C. Johns, M. Noël, *J. Mol. Spectrosc.* 173 (1995) 55–61.
- [30] J. Orphal, Q. Kou, F. Kwabia Tchana, O. Pirali, J.-M. Flaud, *J. Mol. Spectrosc.* 221 (2003) 239–243.
- [31] J.-M. Flaud, M. Birk, G. Wagner, S. Klee, G. Chr. Mellau, J. Orphal, W.J. Lafferty, *J. Mol. Spectrosc.* 191 (1998) 362–367.
- [32] J.W.C. Johns, *J. Opt. Soc. Am.*, B 2 (1985) 1340–1355.
- [33] G. Guelachvili, M. Birk, Ch.J. Bordé, J.W. Brault, L.R. Brown, B. Carli, A.R.H. Cole, K.M. Evenson, A. Fayt, D. Hausmann, J.W.C. Johns, J. Kauppinen, Q. Kou, A.G. Maki, K. Narahari Rao, R.A. Toth, W. Urban, A. Valentin, J. Vergès, G. Wagner, M.H. Wappelhorst, J.S. Wells, B.P. Winnewisser, M. Winnewisser, *J. Mol. Spectrosc.* 177 (1996) 164–179.
- [34] J.K.G. Watson, Aspects of Quartic and Sextic Centrifugal Effects on Rotational Energy Levels in: J.R. Durig (Ed.), *Vibrational Spectra and Structure*, Elsevier Ltd., Amsterdam/New York, 1977, pp. 1–9.
- [35] C. Camy-Peyret, J.-M. Flaud, *Vibration-Rotation Dipole Moment Operator for Asymmetric Rotors in: K.N. Rao (Ed.), Molecular Spectroscopy: Modern Research vol. 3*, Academic Press, New York, 1985, pp. 69–110.
- [36] M.A.H. Smith, C.P. Rinsland, V.M. Devi, L.S. Rothman, K.N. Rao, Intensities and Collision-Broadening Parameters from Infrared Spectra: an Update in: K.N. Rao, A. Weber (Eds.), *Spectroscopy of the Earth's Atmosphere and Interstellar Medium*, Academic Press, New York, 1992, pp. 153–260.
- [37] L. S. Rothman, D. Jacquemart, A. Barbe, D. Chris Benner, M. Birk, L.R. Brown, M.R. Carleer, C. Chackerian, Jr., K.V. Chance, V. Dana, V.M. Devi, J.-M. Flaud, R.R. Gamache, A. Goldman, J.-M. Hartmann, K.W. Jucks, A.G. Maki, J.-Y. Mandin, S.T. Massie, J. Orphal, A. Perrin, C.P. Rinsland, M.A.H. Smith, J. Tennyson, R.N. Tolchenov, R.A. Toth, J. Vander Auwera, P. Varanasi, G. Wagner, *The HITRAN 2004 Molecular Spectroscopic Database*, *J. Quant. Spectrosc. Rad. Transfer*, in press.